

# Low-temperature epitaxy of transferable high-quality Pd(111) films on hybrid graphene/Cu(111) substrate

Zhihong Zhang<sup>1,2</sup>, Xiaozhi Xu<sup>1,3</sup>, Ruixi Qiao<sup>1</sup>, Junjiang Liu<sup>4</sup>, Yuxia Feng<sup>1</sup>, Zhibin Zhang<sup>1</sup>, Peizhao Song<sup>1</sup>, Muhong Wu<sup>1,5</sup>, Lan Zhu<sup>6</sup>, Xuelin Yang<sup>1</sup>, Peng Gao<sup>1</sup>, Lei Liu<sup>4</sup>, Jie Xiong<sup>7</sup>, Enge Wang<sup>1,2,5</sup>, and Kaihui Liu<sup>1</sup> (✉)

<sup>1</sup> State Key Laboratory for Mesoscopic Physics, International Centre for Quantum Materials, Collaborative Innovation Centre of Quantum Matter, School of Physics, Academy for Advanced Interdisciplinary Studies, Peking University, Beijing 100871, China

<sup>2</sup> Physical Science Laboratory, Huairou National Comprehensive Science Centre, Beijing 101400, China

<sup>3</sup> School of Physics and Telecommunication Engineering, South China Normal University, Guangzhou 510631, China

<sup>4</sup> Department of Materials Science and Engineering, College of Engineering, Peking University, Beijing 100871, China

<sup>5</sup> Songshan Lake Materials Laboratory, Institute of Physics, Chinese Academy of Sciences, Guangdong 523808, China

<sup>6</sup> Peking Union Medical College Hospital, Beijing 100730, China

<sup>7</sup> State Key Laboratory of Electronic Thin Films and Integrated Devices, University of Electronic Science and Technology of China, Chengdu 610054, China

© Tsinghua University Press and Springer-Verlag GmbH Germany, part of Springer Nature 2019

Received: 5 June 2019 / Revised: 9 August 2019 / Accepted: 15 August 2019

## ABSTRACT

The continuous pursuit of miniaturization in the electronics and optoelectronics industry demands all device components with smaller size and higher performance, in which thin metal film is one heart material as conductive electrodes. However, conventional metal films are typically polycrystalline with random domain orientations and various grain boundaries, which greatly degrade their mechanical, thermal and electrical properties. Hence, it is highly demanded to produce single-crystal metal films with epitaxy in an appealing route. Traditional epitaxy on non-metal single-crystal substrates has difficulty in exfoliating away due to the formation of chemical bonds. Newly developed epitaxy on single-crystal graphene enables the easy exfoliation of epilayers but the annealing temperature must be high (typical 500–1,000 °C and out of the tolerant range of integrated circuit technology) due to the relative weak interfacial interactions. Here we demonstrate the facile production of 6-inch transferable high-quality Pd(111) films on single-crystal hybrid graphene/Cu(111) substrate with CMOS-compatible annealing temperature of 150 °C only. The interfacial interaction between Pd and hybrid graphene/Cu(111) substrate is strong enough to enable the low-temperature epitaxy of Pd(111) films and weak enough to facilitate the easy film release from substrate. The obtained Pd(111) films possess superior properties to polycrystalline ones with ~ 0.25 eV higher work function and almost half sheet resistance. This technique is proved to be applicable to other metals, such as Au and Ag. As the single-crystal graphene/Cu(111) substrates are obtained from industrial Cu foils and accessible in meter scale, our work will promote the massive applications of large-area high-quality metal films in the development of next-generation electronic and optoelectronic devices.

## KEYWORDS

single-crystal metal film, graphene/Cu(111) substrate, interfacial interactions, meter scale

## 1 Introduction

Metal materials play an irreplaceable role in modern silicon (Si)-based complementary metal-oxide-semiconductor (CMOS) technology as conductive electrodes. Unlike the utilization of high-quality single-crystal Si as semiconductor materials, currently used thin metal films, typically produced by deposition or sputtering, are polycrystalline with random domain orientations and lots of defective grain boundaries, which degrade their mechanical, thermal and electronic properties significantly [1–3]. For electronic and optoelectronic applications, to achieve higher integration and better performance, thin single-crystal metal films with high quality are strongly desired [4–6]. The single-crystal metal films can be in principle achieved by the epitaxy on other single-crystal substrates, such as Si, sapphire, mica or other metals [7–13]. However, the expensive price and small size of conventional single-crystal substrates restrain their large-scale production and wide applications. Additionally, it is very difficult to exfoliate the epitaxial thin metal films from these substrates, as

they will form strong chemical bonds at their interface.

Graphene, with well-ordered hexagonal structure, possesses excellent mechanical and thermal properties, the best atomic flatness and high chemical stabilities, and thus is considered as an ideal substrate for epitaxy [14–19]. Especially, there are no dangling bonds in the surface of graphene and the epitaxy is mediated by the weak van der Waals (vdW) interaction, which leads to relaxed lattice matching and facile release of epilayers [20–22]. Thanks to the great progress in graphene growth, the preparation of large-area single-crystal graphene comes into reality [23–27], and thus it becomes realistic to realize the large-scale epitaxy of thin films on graphene. It has been widely demonstrated that single-crystal graphene films can be epitaxially grown on single-crystal metal substrate, like Ru(0001), Cu (111), Ir(111) and Pt(111) [28–31]; in reverse, the metal single crystals might be achievable on single-crystal graphene films. It was reported that several face centered cubic (fcc) metals (like Ni, Cu, Pt and Au) deposited onto graphene exhibit (111) out-of-plane orientation after thermal annealing [32, 33]. However, the very

weak vdW interaction between graphene and metals typically requires a very high annealing temperature (500–1,000 °C) to realize the epitaxy of high-quality metal films, which is incompatible with current CMOS technology (the upper limit annealing temperature for metal is  $\sim 450$  °C). Therefore, to develop a low-temperature epitaxy technique to produce large single-crystal metal films with easy exfoliation ability is highly demanded.

The low-temperature epitaxy of transferable thin metal films seems in a dilemma that strong interfacial interaction is required to realize low-temperature epitaxy, while weak coupling strength is preferred to achieve facile epilayer release. In this work, we utilized a hybrid substrate, single-crystal graphene/Cu(111), a commensurate system with graphene and Cu(111) of matched symmetry and lattice orientation, to realize the low-temperature epitaxy of transferrable high-quality palladium (Pd) films. The cooperative effects of graphene and Cu(111) are strong enough to induce the epitaxy of high-quality Pd(111) films with post-annealing temperature at 150 °C only. On the other hand, the existence of graphene between Pd(111) film and Cu(111) enables the easy release of epitaxial metal films. With this substrate, the epitaxy of other metals like Au and Ag has also been successfully achieved. As the designed single-crystal graphene/Cu(111) substrate can be obtained from commercial polycrystalline Cu foils at meter scale and with low cost [26], our work provides an avenue to realize the economical fabrication of large-area high-quality thin metal films and thus will promote their massive applications in the development of high-performance electronic and optoelectronic devices with smaller size.

## 2 Results and discussions

The key epitaxial processes are schematically shown in Fig. 1(a). The polycrystalline Cu foil was first transformed into single-crystal Cu(111) by our designed temperature-gradient-driven thermal annealing process and then served as substrate to epitaxially grow single-crystal graphene film by chemical vapor deposition (CVD) method (see Experimental section for details) [26]. Figure 1(b) gives a photograph of single-crystal Cu(111) with size about 15 cm  $\times$  15 cm after mild oxidation (the right dark regions near the edge are polycrystalline) [34]. Afterwards Pd was deposited onto graphene/Cu(111) by electron beam evaporation with different film thickness.

As limited by the space of our deposition chamber, currently the size of the epitaxial Pd film reaches maximum of 6 inches, as shown in Fig. 1(c). Post-annealing under low temperature of 150 °C was carried out to improve the film quality (Fig. S1 in the Electronic Supplementary Material (ESM)). Graphene can act as an efficient separation between Pd and Cu, without which the Pd will easily alloy with Cu (Fig. S2 in the ESM) [35]. The Pd films can be separated from Cu foil by exfoliation using thermal released tape or directly etching the Cu foils. Figure 1(d) shows the Pd film supported by thermal released tape after exfoliation from the substrate.

We use X-ray diffraction (XRD) to characterize the crystallographic properties of epitaxial Pd film (50 nm in thickness) on graphene/Cu(111) after thermal annealing. The XRD  $2\theta$  scan result (Fig. 2(a)) shows that the Pd film only has (111) and (222) peaks, indicating that Pd has a high (111) out-of-plane order. In addition, the azimuthal off-axis  $\phi$  scan (Fig. 2(b)) gives six-fold symmetry of the diffraction peaks corresponding to Pd(200) with 60° intervals, implying that there is only 180° in-plane rotation of Pd grains, as the single-crystal Pd(111) should have three-fold symmetry [5]. We employed the intensity and full width at half maxima (FWHM) of the (111) peak to characterize the crystalline quality of the films. Figure 2(c) shows high resolution XRD (HRXRD) curves corresponding to the (111) peaks of Pd films with thickness of 10, 20, 30, 40, 50 and 100 nm, respectively, and insert is the FWHM of the peaks. It is clear that the intensity increases and FWHM decreases with thickness increment, demonstrating improved crystalline quality of thicker Pd film within thickness of at least 100 nm.

To have deeper insight into the epitaxial structure, we applied high-resolution transmission electron microscopy (HRTEM) to study the lattice orientation relation between Pd and graphene/Cu(111) before the formation of continuous film. We deposited  $\sim 2$  nm thick Pd on graphene/Cu(111), then transferred the Pd/graphene film onto TEM grid. In the low magnification TEM image (Fig. 2(d)) it can be seen that the Pd forms dendrite structure (the dark area indicated by the orange arrow). In the selected area electron diffraction (SAED) pattern (Fig. 2(e)), the diffraction spots of graphene can be clearly identified in the purple circles. The Pd diffraction patterns are aligned with graphene, revealing an epitaxial growth of Pd on graphene ( $\sim 5^\circ$  variation of Pd diffraction points was observed due to the relative low quality of discontinuous thin Pd film, which is

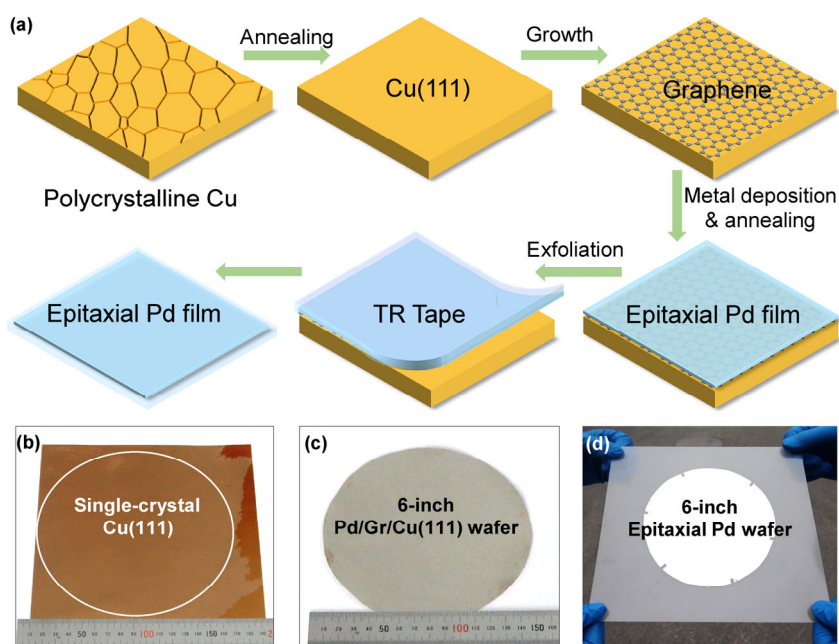


**Figure 1** Preparation of transferable 6-inch Pd films. (a) Schematics of key epitaxial processes. Photographs of 6-inch single-crystal Cu(111) (b), Pd film deposited on graphene/Cu(111) (c) and Pd film supported by thermal released tape (d).

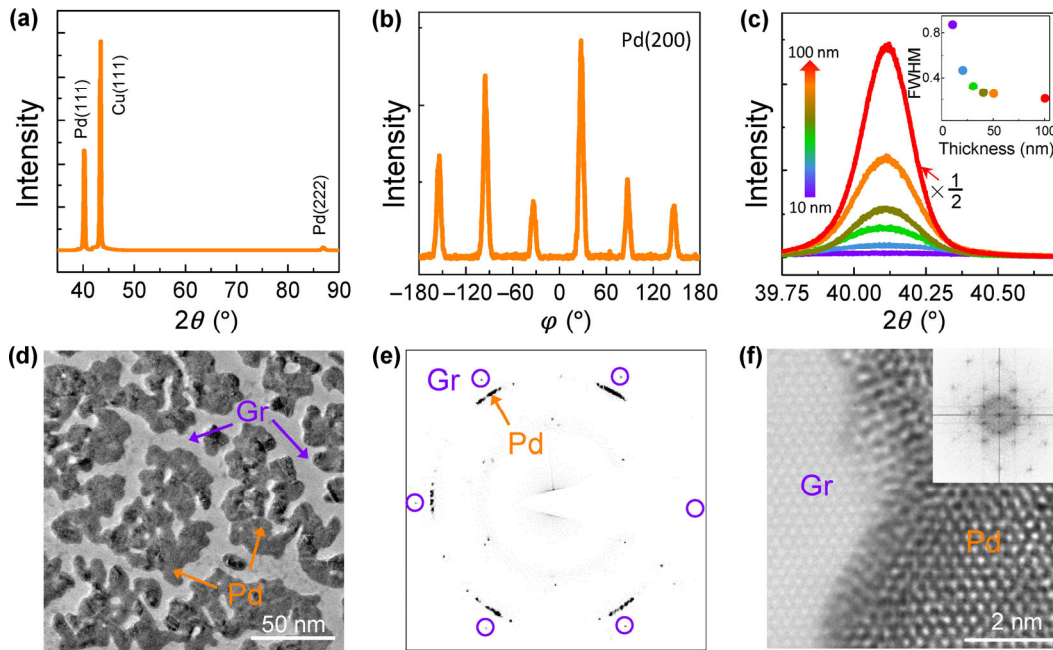


**Figure 2** Crystallographic characterization and epitaxial relation of the Pd films on graphene/Cu(111). (a) XRD  $2\theta$  scan spectrum with only (111) and (222) peaks of Pd, indicating a high (111) out-of-plane order. (b) XRD azimuthal off-axis  $\varphi$  scan spectrum. The six-fold symmetry of the diffraction peaks corresponding to Pd(200) with  $60^\circ$  intervals, implies that there is only  $180^\circ$  in-plane rotation of Pd grains. (c) HRXRD  $2\theta$  scan results of Pd films with different thickness. Inset: corresponding FWHM of the (111) peaks. Low magnification TEM image (d), SAED pattern (e) and HRTEM image (f) of  $\sim 2$  nm thick Pd on single-crystal graphene film. Inset in (f): fast Fourier transformation pattern of the HRTEM image. The parallel lattice of graphene and Pd demonstrates the epitaxy of Pd on graphene/Cu(111).

consistent with previous observation that the continuous epitaxy film has higher quality than discontinuous one [36]). This lattice alignment between Pd and graphene is further consolidated by the HRTEM image shown in Fig. 2(f). As graphene is well aligned with single-crystal Cu(111) (Fig. S3 in the ESM), the lattices of Pd(111), graphene and Cu(111) all have the same alignment.

It is quite clear that Pd film can be epitaxial grown on graphene/Cu(111) surface. Then a natural question about the epitaxy is whether the epitaxial behavior of Pd is determined by graphene, Cu(111) or both. Previous study has manifested that the potential field of the strong polarized substrate can penetrate monolayer graphene and interact with the epilayers [20, 21]. To figure out the roles of Cu(111) in our experiments we carried out control

experiments of the deposition behaviors of Pd on different substrates, i.e.,  $300\text{ nm SiO}_2/\text{Si}$ , graphene and graphene/Cu(111). For each sample, the thickness of Pd film is fixed as 100 nm and the orientation information of the Pd films on different substrates was analyzed by the electron back-scattered diffraction (EBSD) technique. The inverse pole figure (IPF) maps (Figs. 3(a)–3(c)) and (001) pole figures (using a single point per grain weighted by size) (Figs. 3(e)–3(g)) were used to check the crystallographic features of Pd films. It is demonstrated that,  $\text{SiO}_2/\text{Si}$  has no effect on epitaxy and induces polycrystalline film (Figs. 3(a) and 3(e)), pure graphene substrate can lead epitaxy but with half domains of  $180^\circ$  in-plane rotation (Figs. 3(b) and 3(f)), and hybrid graphene/Cu(111) substrate can lead nice epitaxy with very few  $180^\circ$  in-plane domain rotation (Figs. 3(c) and 3(g)). The

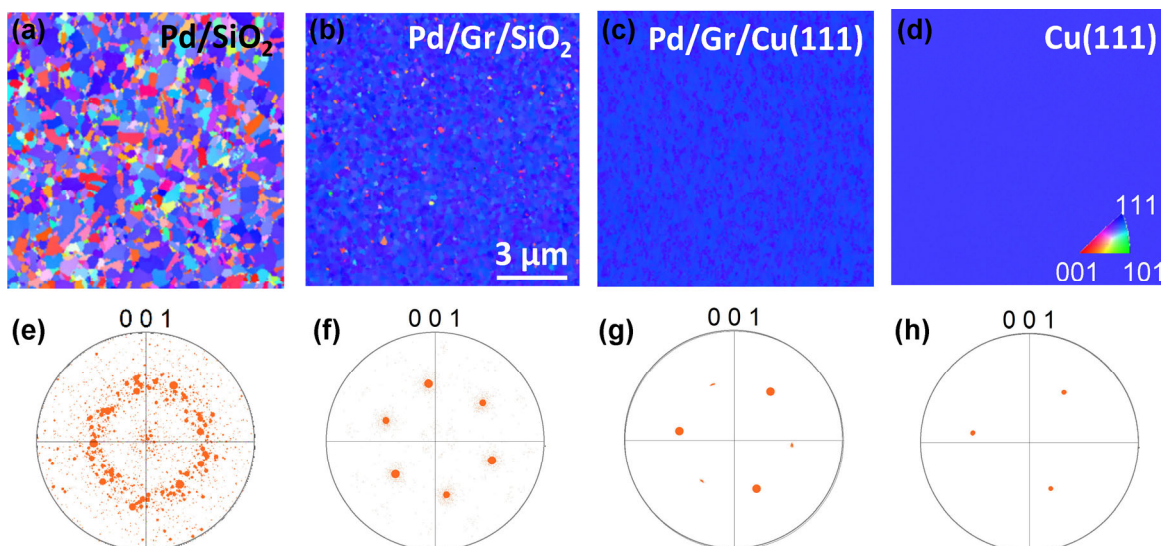


**Figure 3** Deposition behaviors of Pd on different substrates. EBSD IPF maps of Pd deposited on  $300\text{ nm SiO}_2/\text{Si}$  (a), single-crystal graphene film (b) and single-crystal graphene/Cu(111) (c), and the underlying single-crystal Cu(111) (d). The complete (111) orientation in (c) demonstrates the high quality of the epitaxial Pd film on graphene/Cu(111). (e)–(h) The corresponding (001) pole figures of (a)–(d) using a single point per grain weighted by size. The dominant orientation in Pd film (g) is perfectly parallel with that of Cu(111) (h).

dominant orientation in Pd films on graphene/Cu(111) is exactly the same with that of underlying Cu(111) (Figs. 3(d) and 3(h)). These observations verified that the Cu(111) is the main driving force to form ideal Pd epitaxy on the hybrid graphene/Cu(111) substrate. Although metal Cu is nonpolar, its potential should penetrate monolayer graphene more or less and affect the epitaxial behaviour of Pd films. Additionally, graphene films are epitaxially grown on Cu(111), thus they can form a commensurate system with a hexagonal Moiré pattern [37]. The formation of Moiré pattern may also contribute to the epitaxial deposition of metal films. Besides, due to the different work function of graphene and Cu(111), there is charge transfer between them and a dipole perpendicular to the interface is formed [38]. This dipole may be beneficial to the epitaxial deposition.

The obtained Pd(111) films are close to ideal single crystal and their properties are supposed superior to the polycrystalline ones. We first explored their difference on work function. Pd is of high work function and widely used as electrode material to fabricate p-type field-effect transistors [3]. For this kind of device applications, higher work function is under pursuit. It was demonstrated that single-crystal Pd(111) has higher work function ( $\sim 5.6$  eV) than polycrystalline one ( $\sim 5.22$  eV) [39]. Here we utilized the Kelvin probe force microscope (KPFM) to obtain the work function information of Pd film. Figures 4(a) and 4(b) give the morphology and surface potential of Pd(111) on SiO<sub>2</sub>/Si. In KPFM measurement

the potential is defined as  $V = \frac{\phi_{\text{tip}} - \phi_{\text{sample}}}{-e}$ , where  $\phi_{\text{tip}}$  and  $\phi_{\text{sample}}$  are

the work functions of tip and sample, respectively, and  $e$  is the electron charge. This means that a surface with higher work function should exhibit higher potential. The base line difference in Fig. 4(c) shows that our Pd(111) film has  $\sim 0.25$  V higher potential than polycrystalline one (The potential peaks in Fig. 4(c) are due to the discontinuity at the edge of Pd films). Surface morphology map and potential map of polycrystalline Pd films are shown in Fig. S4 in the ESM. Besides work function, we also evaluated the electrical conducting properties of the thin Pd films on thermal released tapes. The average sheet

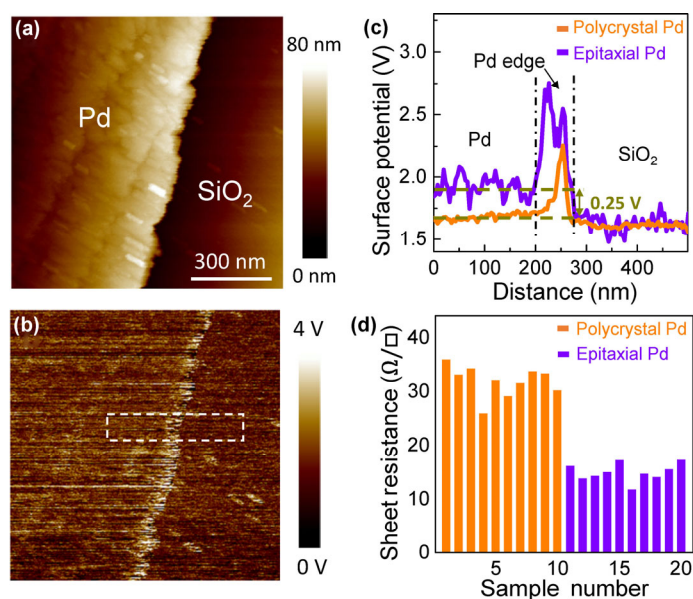


**Figure 4** Electrical properties characterization of epitaxial Pd films. Height map (a) and surface potential map (b) of Pd(111) film transferred onto SiO<sub>2</sub>/Si substrate obtained by KPFM. (c) Line profiles of surface potential of Pd(111) film (purple curve) and polycrystalline one (orange curve). The base line difference shows Pd(111) film has  $\sim 0.25$  V higher potential than polycrystalline one. The potential peaks are due to the discontinuity at the edge of Pd films. (d) Sheet resistance of polycrystalline Pd and Pd(111) films. The sheet resistance of Pd(111) films is about half of that of polycrystalline ones.

resistance of Pd(111) film with thickness of 50 nm is  $15 \Omega/\square$ , half of the polycrystalline one with the same thickness (Fig. 4(d)). This greatly improved conductivity can be attributed to the high quality of our Pd(111) film. One note is that although the epitaxial Pd film have fewer 180° rotated domains, this type of 180° domain boundaries is quite unique in terms that they contribute very small grain boundary resistance [1].

This hybrid graphene/Cu(111) substrate can be widely applicable to epitaxially grow other metal films. We show Au and Ag can also form highly (111)-oriented films on graphene/Cu(111) (Figs. 5(a) and 5(b)). Similar to Pd films, Au films are composed of complete (111) grains (Fig. 5(c)), while in Ag films, there are a small amount of grains with other orientations (Fig. 5(d)). We also deposit Au and Ag on single-crystal graphene films transferred onto 300 nm SiO<sub>2</sub>/Si. In that case, Au films are still (111) oriented while Ag films are polycrystalline (Fig. S5 in the ESM). This result implies that the interactions between Ag and graphene/Cu(111) are weaker, in consistent with previous understanding [40]. The annealing temperature here is also as low as 150 °C.

### 3 Conclusions

In summary, we demonstrate the low-temperature epitaxy of transferable high-quality Pd(111), Au(111) and Ag(111) films on hybrid graphene/Cu(111) substrate. In this hybrid substrate Cu(111) serves as the main origin to drive low-temperature epitaxy, while graphene is the critical buffer layer to realize easy film exfoliation. Nowadays, it is mature to produce meter-scale single-crystal graphene/Cu(111) from industrial polycrystalline Cu foils and thus this single-crystal hybrid substrate is quite easily accessible. Our results should stimulate the immediate massive applications of large-area high-quality metal films in the development of next-generation electronic and optoelectronic devices.

### 4 Experimental

#### 4.1 Annealing of single-crystal Cu foils and growth of single-crystal graphene films

The annealing of commercial Cu foils was carried out in a home-build

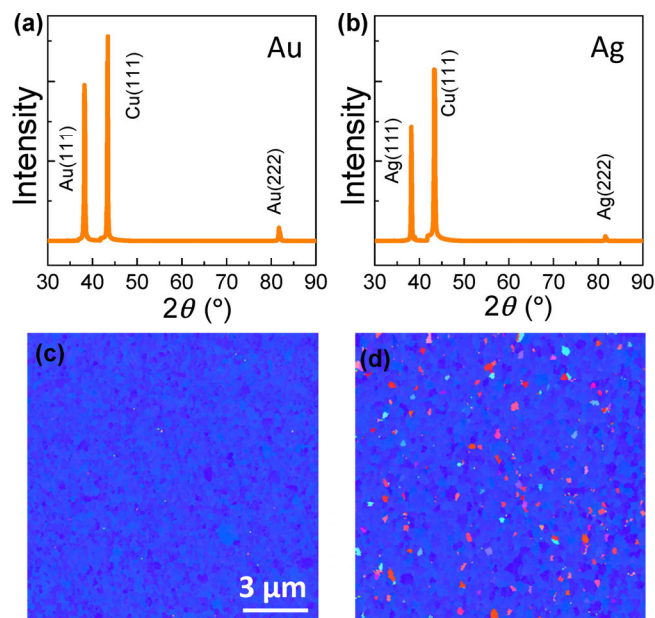


**Figure 5** Epitaxy of Au and Ag films on single-crystal graphene/Cu(111). (a) and (c) XRD spectrum and EBSD IPF map for Au deposited on graphene/Cu(111). (b) and (d) XRD spectrum and EBSD IPF map for Ag deposited on graphene/Cu(111).

CVD system (10 inch in diameter). The central region of the furnace was first heated up to 1,030 °C with 800 sccm Ar and then kept at 1,030 °C for 1 h with 800 sccm Ar and 50 sccm H<sub>2</sub>. After the annealing process, CH<sub>4</sub> as carbon precursor was introduced into the system to grow graphene. The whole process was performed under ambient pressure.

## 4.2 Characterization

XRD measurements were conducted using a PANalytical X'Pert Pro system. EBSD characterizations were obtained by PHI 710 scanning Auger electron spectrometer with an EBSD detector and the data are processed by the software OIM analysis. HRTEM and SAED experiments were performed in Titan Themis G2 300 operated at 80 and 300 kV respectively. LEED measurements were performed using Omicron LEED system in UHV with base pressure <math>3 \times 10^{-7}</math> Pa. The surface potential was measured with Bruker Dimension ICON Scanasyt in the mode of Frequency Modulation KPFM. The room temperature sheet resistance of the Pd films was measured based on the four-point probe method to eliminate contact resistance. Each data is obtained from a 1 mm × 1 mm area.

## Acknowledgements

This work was supported by the National Key R&D Program of China (Nos. 2016YFA0300903 and 2016YFA0300804), the National Natural Science Foundation of China (NSFC) (No. 11888101), the National Equipment Program of China (No. ZDYZ2015-1), Beijing Graphene Innovation Program (No. Z181100004818003), Beijing Municipal Science & Technology Commission (No. Z181100004218006), Bureau of Industry and Information Technology of Shenzhen (Graphene platform contract NO. 201901161512), and the Key R&D Program of Guangdong Province (No. 2019B010931001).

**Electronic Supplementary Material:** Supplementary material (more characterization results of Pd films, LEED patterns of graphene and Cu(111) and XRD results for Au and Ag films deposited on graphene) is available in the online version of the article at <https://doi.org/10.1007/s12274-019-2503-8>.

## References

- Lu, L.; Shen, Y. F.; Chen, X. H.; Qian, L. H.; Lu, K. Ultrahigh strength and high electrical conductivity in copper. *Science* **2004**, *304*, 422–426.
- Lu, K.; Lu, L.; Suresh, S. Strengthening materials by engineering coherent internal boundaries at the nanoscale. *Science* **2009**, *324*, 349–352.
- Liu, Y.; Guo, J.; Zhu, E. B.; Liao, L.; Lee, S. J.; Ding, M. N.; Shakir, I.; Gambin, V.; Huang, Y.; Duan, X. F. Approaching the Schottky-Mott limit in van der Waals metal-semiconductor junctions. *Nature* **2018**, *557*, 696–700.
- Wu, Y.; Xiang, J.; Yang, C.; Lu, W.; Lieber, C. M. Single-crystal metallic nanowires and metal/semiconductor nanowire heterostructures. *Nature* **2004**, *430*, 61–65.
- Mahenderkar, N. K.; Chen, Q. Z.; Liu, Y. C.; Duchild, A. R.; Hofheins, S.; Chason, E.; Switzer, J. A. Epitaxial lift-off of electrodeposited single-crystal gold foils for flexible electronics. *Science* **2017**, *355*, 1203–1206.
- Zhang, K.; Pitner, X. B.; Yang, R.; Nix, W. D.; Plummer, J. D.; Fan, J. A. Single-crystal metal growth on amorphous insulating substrates. *Proc. Natl. Acad. Sci. USA* **2018**, *115*, 685–689.
- Grünbaum, E. Epitaxial growth of metal single-crystal films. *Vacuum* **1974**, *24*, 153–164.
- Winau, D.; Koch, R.; Führmann, A.; Rieder, K. H. Film growth studies with intrinsic stress measurement: Polycrystalline and epitaxial Ag, Cu, and Au films on Mica(001). *J. Appl. Phys.* **1991**, *70*, 3081–3087.
- Ago, H.; Ito, Y.; Mizuta, N.; Yoshida, K.; Hu, B. S.; Orofeo, C. M.; Tsuji, M.; Ikeda, K. I.; Mizuno, S. Epitaxial chemical vapor deposition growth of single-layer graphene over cobalt film crystallized on sapphire. *ACS Nano* **2010**, *4*, 7407–7414.
- Miller, D. L.; Keller, M. W.; Shaw, J. M.; Chiamonti, A. N.; Keller, R. R. Epitaxial (111) films of Cu, Ni, and Cu<sub>x</sub>Ni<sub>y</sub> on  $\alpha$ -Al<sub>2</sub>O<sub>3</sub> (0001) for graphene growth by chemical vapor deposition. *J. Appl. Phys.* **2012**, *112*, 064317.
- Hu, B. S.; Ago, H.; Ito, Y.; Kawahara, K.; Tsuji, M.; Magome, E.; Sumitani, K.; Mizuta, N.; Ikeda, K. I.; Mizuno, S. Epitaxial growth of large-area single-layer graphene over Cu(111)/sapphire by atmospheric pressure CVD. *Carbon* **2012**, *50*, 57–65.
- Walker, E. S.; Na, S. R.; Jung, D.; March, S. D.; Kim, J. S.; Trivedi, T.; Li, W.; Tao, L.; Lee, M. L.; Liechti, K. M. et al. Large-area dry transfer of single-crystalline epitaxial bismuth thin films. *Nano Lett* **2016**, *16*, 6931–6938.
- Kelso, M. V.; Tubbesing, J. Z.; Chen, Q. Z.; Switzer, J. A. Epitaxial electrodeposition of chiral metal surfaces on silicon(643). *J. Am. Chem. Soc.* **2018**, *140*, 15812–15819.
- Huang, X.; Li, S. Z.; Huang, Y. Z.; Wu, S. X.; Zhou, X. Z.; Li, S. Z.; Gan, C. L.; Boey, F.; Mirkin, C. A.; Zhang, H. Synthesis of hexagonal close-packed gold nanostructures. *Nat. Commun.* **2011**, *2*, 292.
- Liu, Z.; Song, L.; Zhao, S. Z.; Huang, J. Q.; Ma, L. L.; Zhang, J. N.; Lou, J.; Ajayan, P. M. Direct growth of graphene/hexagonal boron nitride stacked layers. *Nano Lett.* **2011**, *11*, 2032–2037.
- Shi, Y. M.; Zhou, W.; Lu, A. Y.; Fang, W. J.; Lee, Y. H.; Hsu, A. L.; Kim, S. M.; Kim, K. K.; Yang, H. Y.; Li, L. J. et al. van der Waals epitaxy of MoS<sub>2</sub> layers using graphene as growth templates. *Nano Lett.* **2012**, *12*, 2784–2791.
- Kim, J.; Bayram, C.; Park, H.; Cheng, C. W.; Dimitrakopoulos, C.; Ott, J. A.; Reuter, K. B.; Bedell, S. W.; Sadana, D. K. Principle of direct van der Waals epitaxy of single-crystalline films on epitaxial graphene. *Nat. Commun.* **2014**, *5*, 4836.
- Kim, K. L.; Lee, W.; Hwang, S. K.; Joo, S. H.; Cho, S. M.; Song, G.; Cho, S. H.; Jeong, B.; Hwang, I.; Ahn, J. H. et al. Epitaxial growth of thin ferroelectric polymer films on graphene layer for fully transparent and flexible nonvolatile memory. *Nano Lett.* **2016**, *16*, 334–340.
- Solís-Fernández, P.; Bissett, M.; Ago, H. Synthesis, structure and applications of graphene-based 2D heterostructures. *Chem. Soc. Rev.* **2017**, *46*, 4572–4613.
- Kim, Y.; Cruz, S. S.; Lee, K.; Alawode, B. O.; Choi, C.; Song, Y.; Johnson, J. M.; Heidelberger, C.; Kong, W.; Choi, S. et al. Remote epitaxy through graphene enables two-dimensional material-based layer transfer. *Nature* **2017**, *544*, 340–343.
- Kong, W.; Li, H. S.; Qiao, K.; Kim, Y.; Lee, K.; Nie, Y. F.; Lee, D.; Osadchy, T.; Molnar, R. J.; Gaskill, D. K. et al. Polarity governs atomic interaction through two-dimensional materials. *Nat. Mater.* **2018**, *17*, 999–1004.
- Qi, Y.; Wang, Y. Y.; Pang, Z. Q.; Dou, Z. P.; Wei, T. B.; Gao, P.; Zhang, S. S.; Xu, X. Z.; Chang, Z. H.; Deng, B. et al. Fast growth of strain-free AlN on graphene-buffered sapphire. *J. Am. Chem. Soc.* **2018**, *140*, 11935–11941.
- Li, X. S.; Cai, W. W.; An, J. H.; Kim, S.; Nah, J.; Yang, D. X.; Piner, R.; Velamakanni, A.; Jung, I.; Tutuc, E. et al. Large-area synthesis of high-quality and uniform graphene films on copper foils. *Science* **2009**, *324*, 1312–1314.
- Gao, L. B.; Ren, W. C.; Xu, H. L.; Jin, L.; Wang, Z. X.; Ma, T.; Ma, L. P.; Zhang, Z. Y.; Fu, Q.; Peng, L. M. et al. Repeated growth and bubbling transfer of graphene with millimetre-size single-crystal grains using platinum. *Nat. Commun.* **2012**, *3*, 699.
- Wu, T. R.; Zhang, X. F.; Yuan, Q. H.; Xue, J. C.; Lu, G. Y.; Liu, Z. H.; Wang, H. S.; Wang, H. M.; Ding, F.; Yu, Q. K. et al. Fast growth of inch-sized single-crystalline graphene from a controlled single nucleus on Cu-Ni alloys. *Nat. Mater.* **2016**, *15*, 43–47.
- Xu, X. Z.; Zhang, Z. H.; Dong, J. C.; Yi, D.; Niu, J. J.; Wu, M. H.; Lin, L.; Yin, R. K.; Li, M. Q.; Zhou, J. Y. et al. Ultrafast epitaxial growth of metre-sized single-crystal graphene on industrial Cu foil. *Sci. Bull.* **2017**, *62*, 1074–1080.
- Vlassioug, I. V.; Stehle, Y.; Pudasaini, P. R.; Unocic, R. R.; Rack, P. D.; Baddorf, A. P.; Ivanov, I. N.; Lavrik, N. V.; List, F.; Gupta, N. et al. Evolutionary selection growth of two-dimensional materials on polycrystalline substrates. *Nat. Mater.* **2018**, *17*, 318–322.
- Sutter, P. W.; Flege, J. I.; Sutter, E. A. Epitaxial graphene on ruthenium. *Nat. Mater.* **2008**, *7*, 406–411.
- Coraux, J.; N'Diaye, A. T.; Busse, C.; Michely, T. Structural coherency of graphene on Ir(111). *Nano Lett.* **2008**, *8*, 565–570.

- [30] Gao, M.; Pan, Y.; Huang, L.; Hu, H.; Zhang, L. Z.; Guo, H. M.; Du, S. X.; Gao, H. J. Epitaxial growth and structural property of graphene on Pt(111). *Appl. Phys. Lett.* **2011**, *98*, 033101.
- [31] Nguyen, V. L.; Shin, B. G.; Duong, D. L.; Kim, S. T.; Perello, D.; Lim, Y. J.; Yuan, Q. H.; Ding, F.; Jeong, H. Y.; Shin, H. S. et al. Seamless stitching of graphene domains on polished copper (111) foil. *Adv. Mater.* **2015**, *27*, 1376–1382.
- [32] Kim, D. W.; Kim, S. J.; Choi, H. O.; Jung, H. T. Epitaxial crystallization behaviors of various metals on a graphene surface. *Adv. Mater. Interfaces* **2016**, *3*, 1500741.
- [33] Lu, Z. H.; Sun, X.; Washington, M. A.; Lu, T. M. Quasi van der Waals epitaxy of copper thin film on single-crystal graphene monolayer buffer. *J. Phy. D: Appl. Phys.* **2018**, *51*, 095301.
- [34] Zhang, Z. B.; Xu, X. Z.; Zhang, Z. H.; Wu, M. H.; Wang, J. H.; Liu, C.; Shang, N. Z.; Wang, J. X.; Gao, P.; Yu, D. P. et al. Identification of copper surface index by optical contrast. *Adv. Mater. Interfaces* **2018**, *5*, 1800377.
- [35] Wang, H. Z.; Leong, W. S.; Hu, F. T.; Ju, L. L.; Su, C.; Guo, Y. K.; Li, J.; Li, M.; Hu, A. M.; Kong, J. Low-temperature copper bonding strategy with graphene interlayer. *ACS Nano* **2018**, *12*, 2395–2402.
- [36] Matthews, J. W. *Epitaxial Growth*. Elsevier: Amsterdam, 1975.
- [37] Xu, X. Z.; Yi, D.; Wang, Z. C.; Yu, J. C.; Zhang, Z. H.; Qiao, R. X.; Sun, Z. H.; Hu, Z. H.; Gao, P.; Peng, H. L. et al. Greatly enhanced anticorrosion of Cu by commensurate graphene coating. *Adv Mater* **2018**, *30*, 1702944.
- [38] Giovannetti, G.; Khomyakov, P. A.; Brocks, G.; Karpan, V. M.; van den Brink, J.; Kelly, P. J. Doping graphene with metal contacts. *Phys Rev Lett* **2008**, *101*, 026803.
- [39] Hölzl, J.; Schulte, F. K.; Wagner, H. *Solid Surface Physics*. Springer: Berlin, 1979.
- [40] Liu, X. J.; Wang, C. Z.; Hupalo, M.; Lin, H. Q.; Ho, K. M.; Tringides, M. C. Metals on graphene: Interactions, growth morphology, and thermal stability. *Crystals* **2013**, *3*, 79–111.